Design and Development of Computer-Based Aortic Stenosis Detector Using X-Ray Coronary Angiographic Imaging

Jovem M. Esguerra
Department of Electronics Engineering, Caraga State University (CSU DECE)

Saintrox H. Damian
Department of Electronics Engineering, Caraga State University (CSU DECE)

Engr. Edgardo Ricardo B. Sajonia Jr.
Department of Electronics Engineering, Caraga State University (CSU DECE)

https://doi.org/10.5109/7395583

出版情報：Proceedings of International Exchange and Innovation Conference on Engineering & Sciences (IEICES). 11, pp.653-659, 2025-10-30. International Exchange and Innovation Conference on Engineering & Sciences
バージョン：

Design and Development of Computer-Based Aortic Stenosis Detector Using X-Ray Coronary Angiographic Imaging

Jovem M. Esguerra[1 2], Saintrox H. Damian[1 2], Engr. Edgardo Ricardo B. Sajonia Jr.[123]
[1]Department of Electronics Engineering, Caraga State University (CSU DECE)
[2]College of Engineering and Geosciences, Caraga State University (CSU CEGS)
[3]Center for Renewable Energy, Automation, and Fabrication Technology (CSU CRAFT)
Corresponding author email: ebsajonia@ @carsu.edu.ph

Abstract: *Heart disease is the leading cause of death in the Philippines, with aortic stenosis (AS), a narrowing of the aortic valve, posing serious health risks if undiagnosed. Traditional diagnostic tools like echocardiography and cardiac catheterization are effective but remain costly and inaccessible in many areas. This study introduces a computer based AS detection system using X-ray coronary angiographic (XCA) images, developed primarily in a Python environment. The system follows a pipeline of image preprocessing, vessel segmentation, GAN-based key frame detection, and multiscale CNN classification with GAN-enhanced data augmentation. Implemented using OpenCV, TensorFlow, PyTorch, and MATLAB, the model achieved 93.2% accuracy, 89.5% precision, and a 93.6% F1-score, outperforming baseline approaches. A real-time, Python-MATLAB-based GUI was deployed on a mini-PC to ensure usability and portability. This low-cost, AI-powered solution offers a practical approach to early AS detection, addressing healthcare gaps in the Philippines and supporting more accessible cardiac screening in resource-limited settings.*

Keywords: Aortic stenosis; X-ray coronary angiography (XCA); Computer-based detection system; GAN-based data augmentation; Convolutional neural network (CNN)

1. INTRODUCTION

Cardiovascular diseases, particularly those affecting the heart valves, remain a significant global health concern. Among these, aortic stenosis (AS), characterized by the narrowing of the aortic valve, is a critical condition due to its potential to cause heart failure, arrhythmias, and sudden cardiac death. In AS, the obstructed aortic valve restricts blood flow from the heart, forcing it to work harder. This can lead to heart muscle thickening, reduced blood flow, and eventually, heart failure [1].

Aortic stenosis is commonly caused by age-related calcification, congenital defects, or rheumatic fever, predominantly affecting older adults. Symptoms such as chest pain, fatigue, shortness of breath, and fainting, especially during exertion, highlight the need for timely diagnosis and intervention to prevent life-threatening complications. The increasing incidence of AS with the aging global population underscores the need for efficient, accurate, and accessible diagnostic solutions. While echocardiography and cardiac catheterization are crucial for diagnosis, they have limitations. Echocardiography's accuracy can be affected by suboptimal acoustic windows and operator dependency, potentially leading to misclassification of disease severity. Cardiac catheterization, although providing direct pressure measurements, is invasive and carries risks, making it less suitable for routine evaluation [2].

Advances in medical imaging, especially coronary angiography, have significantly improved the assessment of coronary artery anatomy and function, enabling the detection of conditions like stenosis. These techniques offer high-resolution visualization, but interpretation often requires skilled specialists, making diagnosis time-intensive and subject to inter-observer variability [3]. This challenge has spurred interest in automated detection systems to aid clinicians by improving the speed and accuracy of AS diagnosis.

The integration of medical imaging with artificial intelligence (AI) and machine learning has shown promising potential in enhancing diagnostic capabilities through the analysis of large datasets, leading to more precise and consistent results. A computer-based platform offers a flexible and scalable environment for developing advanced detection systems capable of processing complex medical images. Compared to embedded edge-based solutions, computer-based systems provide greater computational power and expandability, potentially accelerating the development and deployment of high-accuracy diagnostic tools in clinical settings.

This study presents the design and development of a computer-based detection system for aortic stenosis using X-ray coronary angiographic imaging. By employing advanced image processing and machine learning algorithms, the system will analyze coronary images to identify and classify stenotic areas, providing healthcare professionals with a reliable, automated diagnostic aid. This seeks to make AS diagnosis more efficient, cost-effective, and accessible, ultimately improving patient outcomes and enabling better resource allocation within healthcare facilities.

2. RELATED WORKS

Despite current medical recommendations favoring aortic valve replacement (AVR) for severe AS, studies indicate that individuals with less than severe AS may still experience notable symptoms and face a less favorable long-term outlook than previously understood. This condition triggers complex structural changes in the heart muscle, and despite the variability in the progression of valve narrowing, there are currently no effective treatments to halt it. Research suggests that moderate AS is linked to increased mortality rates and a faster progression to severe AS.

Outside of AS, research has explored other forms of vascular narrowing. For instance, Morani et al. [4] observed that over a quarter of patients experienced significant narrowing (greater than 75% stenosis) after receiving cardiac implantable electronic devices (CIEDs). Papafaklis et al. [5] developed a new method to assess the functional impact of coronary artery narrowing. Additionally, Hurford and Rothwell [6] noted that in Caucasian individuals, over 12% showed some degree of narrowing in the coronary arteries, with some studies defining this as a narrowing ranging from 50% to complete blockage. It is crucial to recognize that the specific threshold of 50% narrowing is highlighted in the context of coronary artery stenosis in one study and that the clinical importance of a 50% narrowing can differ based on the specific artery and the patient's overall health.

The CAD-RADS™ (CoronaryArtery Disease – Reporting and Data System) classification provides a standardized approach to reporting coronary artery stenosis based on computed tomography angiography (CTA). The system categorizes coronary artery disease severity from CAD-RADS 0 to CAD-RADS 5, depending on the percentage of maximal coronary stenosis observed. CAD-RADS 0 indicates no detectable coronary artery disease (0% stenosis), requiring no further cardiac testing. CAD-RADS 1 corresponds to minimal non-obstructive disease, with 1–24% stenosis or the presence of plaque without luminal narrowing, also not necessitating additional testing. CAD-RADS 2 represents mild non-obstructive disease with 25–49% stenosis, again without the need for further assessment. CAD-RADS 3 describes moderate stenosis (50–69%) and may warrant functional testing to evaluate ischemic significance. More severe narrowing is classified as CAD-RADS 4, with subcategories 4A and 4B. CAD-RADS 4A includes patients with 70–99% stenosis in one or two coronary vessels, and functional assessment or invasive coronary angiography (ICA) is considered. CAD-RADS 4B applies to those with similar levels of stenosis in three vessels or significant left main artery involvement (≥50%), for which ICA is recommended. Finally, CAD-RADS 5 indicates total occlusion (100% stenosis) and typically prompts ICA and/or viability testing to guide treatment decisions. This structured reporting aids in clinical decision-making and enhances communication between radiologists and referring physicians [7].

2.1 X-ray Coronary Angiographic Imaging

The X-ray coronary angiography (CAG) X-ray coronary angiography (CAG) remains a key imaging modality for diagnosing coronary artery disease, a leading global cause of mortality. CAG enables the visualization of coronary artery morphology through real-time imaging during catheterization, while quantitative coronary angiography (QCA) provides standardized, objective measurements. According to Lansky and Pietras [8], several diagnostic approaches based on QCA have been developed, including angiography-derived fractional flow reserve (FFR). Although noninvasive methods such as Coronary Computed Tomography Angiography (CCTA) have shown strong capabilities in detecting stenosis, XCA remains superior in cases involving high-grade stenosis or severe calcification, providing a more comprehensive view of the coronary vasculature [9].

In clinical settings, if significant arterial blockage is detected during an XCA procedure, an angioplasty can be performed immediately to restore blood flow—an option not available with CCTA. Both diagnostic approaches require contrast dye injection and involve radiation exposure. During an XCA, a contrast agent such as fluorescein is administered through a thin catheter inserted into the bloodstream, typically via the arm or groin. This dye enables visualization of the coronary arteries on X-ray images, allowing clinicians to accurately identify areas of narrowing or blockage. XCA provides real-time imaging and direct access to the coronary vessels, making it the preferred method in acute or high-risk cases. Conversely, CCTA, while non-invasive, is primarily used for initial evaluation and has limited therapeutic capability. Fig.1(a) shows visible stenosis regions marked in green, and Fig.1(b) shows non-stenosis regions marked in red. These X-ray coronary angiograms visually differentiate between stenotic and non-stenotic areas, providing critical context for the automated classification system.

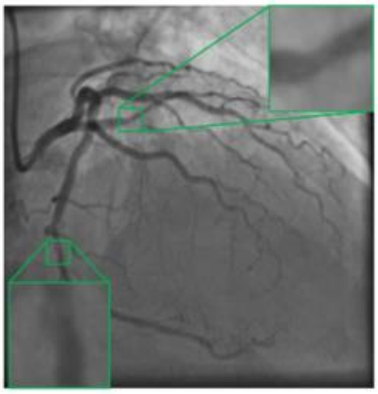

Fig. 1. (a) Stenosis

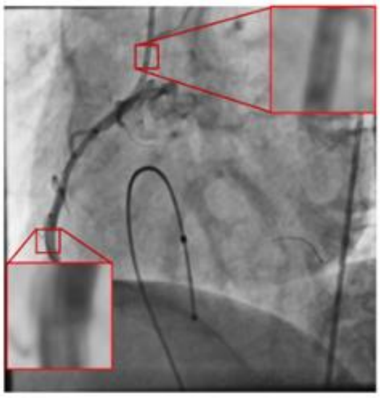

Fig. 1. (b) Non-stenosis

Fig 1. (a) The visible stenosis regions are marked in green, and (b) The non-stenosis regions are marked in red.

3. MATERIALS AND METHODS

This outlines the overall design process, key components, and construction of the computer-based aortic stenosis detection system. It includes system, hardware planning, design, enclosure fabrication, and integration of machine learning architecture to the final prototype.

3.1 Hardware Components Required

To ensure real-time performance and reliability, the system's hardware components were selected for their functionality, compatibility, and durability. Table 1 outlines the key components, highlighting support for efficient image processing, user interaction, and operational stability.

Table 1. Component requirements for hardware design

Hardware Components
1. Minicomputer *(Fast processing power)*
2. Display (touchscreen, compatible with the computer
3. Solid State drive that can cater bulk file of images
4. Cooling fan (compatible with the computer)
5. System enclosure (heat and moisture resistant)
6. Power supply that is enough to supply the whole system

3.2 System Design and Overview

This study employs an Input-Process-Output (IPO) framework for the development and operation of an Aortic Stenosis Detection System utilizing X-ray coronary angiographic (XCA) images (Fig. 2). The input to the system comprises XCA images, which serve as the primary data source for identifying vessel narrowing indicative of aortic stenosis. The process phase encompasses image acquisition and preparation, hardware prototype design, and the development of a machine learning algorithm. This algorithm integrates preprocessing techniques for image enhancement, Geodesic Active Contours (GAC) for vessel segmentation, feature extraction, and a classification model to differentiate between stenotic and non-stenotic cases.

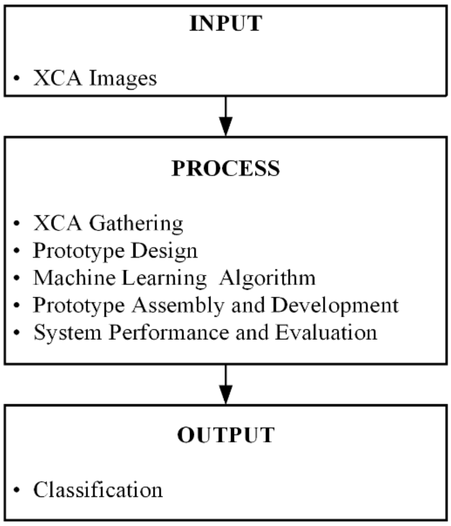

Fig. 2. General framework of the study

Subsequent steps within the process include prototype assembly and rigorous system performance evaluation. The output of the system is a diagnostic classification presented via a user-friendly interface, indicating the presence or absence of stenosis. This output is intended to support clinical decision-making and underscores the potential of the system for scalable deployment in various healthcare settings.

3.3 Block Diagram

The developed aortic stenosis detection system (Fig. 3) initiates its process by loading patient X-ray coronary angiographic (XCA) images from a USB drive into a minicomputer, which functions as the central processing unit. Detection software, executing machine learning algorithms, analyzing these images to identify indicators of aortic stenosis, thereby automating image interpretation. The resulting diagnostic classifications and potential stenotic regions are presented on a 7-inch LCD touchscreen, providing an interactive interface for clinical users. System reliability is maintained through the integration of cooling fans for thermal management and a dedicated power supply. This modular design facilitates deployment in clinical settings, offering a scalable approach to real-time aortic stenosis detection via non-invasive XCA imaging.

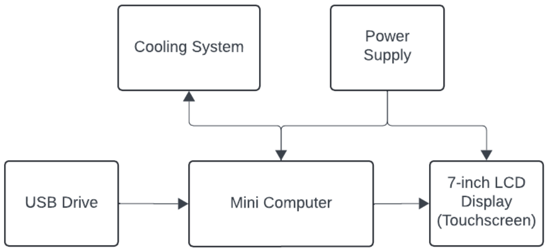

Fig. 3. Block diagram of the system

3.4 Overall System

The flowchart in Fig. 4 outlines the structured methodology employed by the computer-based aortic stenosis detection system for the automated analysis of X-ray coronary angiographic (XCA) images.

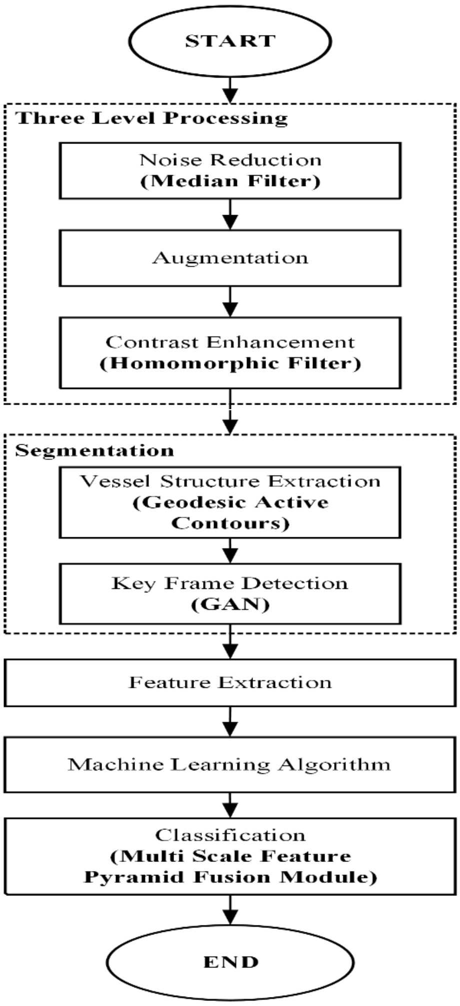

Fig. 4. Flowchart of the system

The XCA image undergoes a three-stage preprocessing pipeline: noise reduction with a median filter, contrast enhancement via a homomorphic filter, and intensity normalization. Vascular structures are then segmented using Geodesic Active Contours (GAC) for precise artery delineation. Key frames are selected using a Generative Adversarial Network (GAN), and features from these frames are extracted and classified to detect stenosis. The system's performance is evaluated using accuracy, sensitivity, precision, and F1-score, showcasing an efficient AI-driven approach to cardiovascular diagnostics.

3.4 Machine Learning Classifier Architecture

Fig. 5. presents an integrated learning architecture designed for classifying coronary artery images into normal and disease-affected categories. The model is based on a Convolutional Neural Network (CNN) backbone with progressive layers (ConY-2 to ConY-5) that extract features from X-ray coronary angiographic images. Early layers detect low-level patterns like edges and contours, while deeper layers identify high-level features such as stenosis.

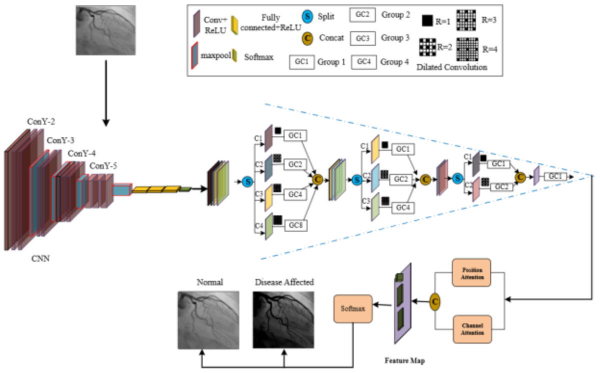

Fig. 5. Classifier learning architecture

Following convolution, the extracted features are flattened and passed through dense layers for classification. A Softmax output layer produces normalized class probabilities:

$$P(y_i) = \frac{e^{z_i}}{\sum_{j=1}^{K} e^{z_j}} \qquad eq.(1)$$

To enhance feature relevance, the model includes two attention mechanisms. *(1) Channel Attention (Mc),* Highlights informative feature maps using pooled statistics and MLPs. *(2) Position Attention (Ms),* Focuses on spatially significant regions via a large 7×7 convolution. Both are applied sequentially to generate refined features:

$$F' = Mc(F) \cdot F,\ F'' = Ms(F') \cdot F' \qquad eq.(2)$$

These enhanced features are classified using:

$$\hat{y} = \operatorname{argmax}(\mathrm{Softmax}(WF''+b)) \qquad eq.(3)$$

A multi-stage fusion mechanism using Graph Convolutional Networks (GCNs: GC1, GC2, GC4, GC8) further captures spatial and relational features from multi-channel inputs. At each stage, feature maps are concatenated, refined, and progressively compressed in a pyramidal structure. Selector nodes apply gating or intermediate Softmax layers to guide feature flow. By combining CNNs, attention, and GCN-based fusion, the model mimics a radiologist's diagnostic workflow, enabling precise coronary artery disease detection.

3.5 Overall Physical Construction

The system enclosure for the aortic stenosis detection system was meticulously designed to provide robust protection and structural integrity, critical for sustained operation. Engineered for optimal airflow, the enclosure effectively regulates internal temperatures, safeguarding components like the Mini PC and SSD from thermal stress, thus enhancing system longevity. Furthermore, it shields against environmental contaminants, ensuring reliable hardware performance.

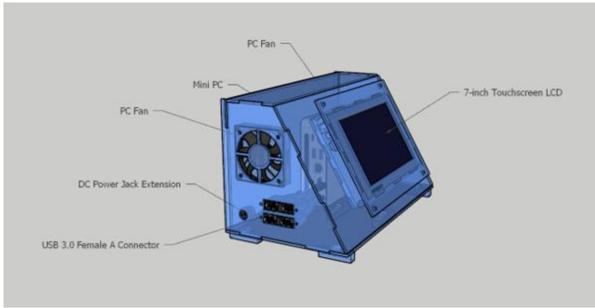

Fig. 6. 3D isometric view of the system prototype

The enclosure features strategically placed ports for easy connectivity and access, along with design elements that support maintenance and upgrades. Made from durable materials, it balances resilience with a professional look suited for clinical and lab use. Its compact, portable design ensures adaptability in various healthcare settings. As shown in Fig. 6, internal components are arranged to optimize functionality, airflow, and accessibility, reflecting a thoughtful, user-centered design.

4. RESULTS AND DISCUSSIONS

This section detailed the development and evaluation of the aortic stenosis detection system, presenting test results, performance metrics, and solutions to implementation challenges

4.1 Software Implementation

The system was designed with a simple graphical user interface (GUI) that allows users to upload X-ray coronary angiographic images, initiate the detection process, and view the diagnostic results (see Fig. 7).

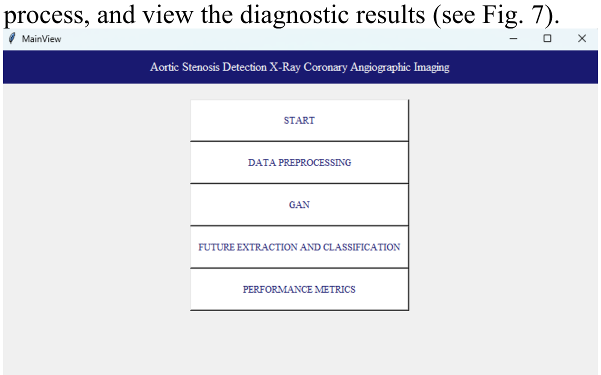

Fig. 7. Graphical user interface of the system

The backend integrates the full image processing pipeline preprocessing, segmentation, and feature extraction followed by the machine learning classification model. Users interact with the system by inserting a USB drive containing the image dataset, selecting the image file through the touchscreen, and viewing the analysis results. The interface was designed to be intuitive, with minimal interaction required from users.

.

4.2 Dataset Summary

The dataset consisted of a total of 3061 images, categorized almost equally between normal and stenosis cases, with 1535 normal and 1526 stenosis images. The majority of the images were sourced from publicly available Kaggle datasets, providing a large volume of annotated coronary angiographic images verified by medical experts. Supplementary datasets from the Philips Allura Xper FD20 system contributed additional clinically acquired images, enhancing the realism and variability of the data. Furthermore, a small number of images were collected from local hospitals within the

Caraga Region under ethical research guidelines, offering a localized clinical perspective (see Table 2). All images were preprocessed to a standardized resolution of 512×512 pixels and stored in PNG format, maintaining high visual quality essential for accurate machine learning analysis. This balanced and clinically verified dataset enabled robust training and validation of the aortic stenosis detection model, supporting both model performance and real-world applicability.

Table 2. Summary of XCA imaging

Source	Total Images	Normal	Stenosis
Philips Allura FD20	49	28	21
Kaggle (Public Dataset)	3000	1500	1500
Local Hospitals (Caraga)	12	7	5
Total	**3061**	**1535**	**1526**

4.3 Confusion Matrix (Original Dataset)

The confusion matrix for the original dataset, offers a detailed overview of the model's classification performance across the two categories: Stenosis and Normal. The model successfully identified 1,209 cases of Stenosis (true positives) and 1,522 cases of Normal (true negatives), reflecting its overall capability in distinguishing between the two classes. However, it also misclassified 317 Normal cases as Stenosis (false positives), and 13 Stenosis cases were incorrectly predicted as Normal (false negatives) (see Fig. 8).

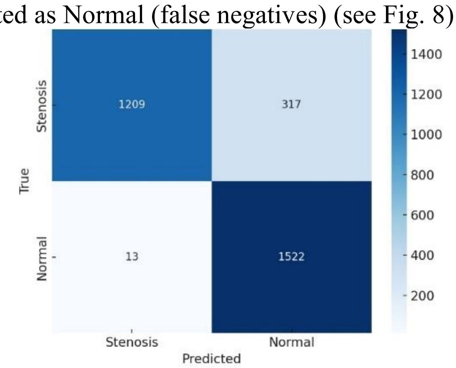

Fig. 8. Confusion matrix for the original dataset

The relatively low number of false negatives indicates that the model is highly effective at detecting Stenosis, an essential trait in medical diagnostics where missing a true positive can have serious consequences. Conversely, the higher count of false positives reflects a tendency to over-predict Stenosis, potentially leading to unnecessary follow-up tests or patient anxiety. This error pattern suggests a conservative bias favoring sensitivity over specificity. While such a bias may be acceptable or even preferred in high-stakes clinical settings, its suitability ultimately depends on the specific diagnostic priorities and risk tolerance of the intended application.

4.4 Performance Metrics (Original Dataset)

The performance metrics for the original dataset highlight the model's strong diagnostic capability. It achieved 89.2% accuracy, with an exceptionally high recall of 0.9894—indicating it correctly identified nearly all true Stenosis cases, crucial in medical settings. However, this high sensitivity came with lower precision (0.7923), meaning around 20.8% of positive predictions were false positives. The F1-score of 0.8800 reflects this balance between recall and precision (see Table 3). Overall, the model excels at detecting Stenosis but could be refined to reduce false positives and improve precision.

Table 3. Performance metrics of the original dataset

Metric	Value
Accuracy	0.8920
Recall	0.9894
Precision	0.7923
F1-score	0.8800

4.5 Application of Augmentation Techniques

The application of rotation, horizontal flipping, and random cropping techniques significantly expanded the size and diversity of the dataset (see Table 4).

Table 4. Summary of data augmentation techniques

Augmentation Method	Applied To	Increase Factor	Remarks
Rotation	All images	3×	±15°, ±30°
Horizontal Flipping	All images	2×	Simulates mirrored anatomical views
Random Cropping	Stenosis cases	2×	Vessel-focused feature enhancement
Brightness Adjustment	All images	1.5×	Simulates variable lighting
Total Generated	All images	~5×	Approx. 15,000 images post-augmentation

The original dataset of ~3,061 images was expanded to over 24,000 through augmentation, introducing greater variability in coronary presentations and imaging conditions. This fivefold increase improved learning stability, reduced overfitting, and enhanced classification accuracy. The enriched dataset enabled better generalization to unseen angiographic images, significantly boosting the model's robustness and overall diagnostic performance.

4.6 Confusion Matrix (Augmented)

The confusion matrices in Fig. 8 and Fig. 9 show notable performance shifts after data augmentation. True Positives rose from 1,209 to 12,291 and True Negatives from 1,522 to 10,533, reflecting improved detection of both Stenosis and Normal cases. Although False Positives and False Negatives also increased—mainly due to the larger dataset—overall performance metrics improved. This indicates that augmentation enhanced the model's generalization despite added complexity, highlighting the need for metric-based evaluation.

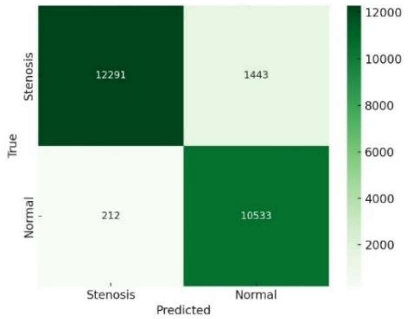

Fig. 9. Confusion matrix for the augmented dataset

4.7 Performance Metrics (Augmented)

Data augmentation led to a notable improvement in classification performance, as shown in Table 5. Accuracy increased from 0.8920 to 0.9324, and precision saw the greatest gain—from 0.7923 to 0.8950, indicating fewer false positives. The F1-score rose from 0.8800 to 0.9358, reflecting a better balance between precision and recall. Although recall slightly decreased from 0.9894 to 0.9830, the model maintained strong sensitivity for detecting Stenosis. Overall, these results confirm that augmentation enhanced the model's robustness, improving both precision and consistency in predictions.

Table 5. Performance metrics of the augmented dataset

Metric	Original	Augmented	Change
Accuracy	0.8920	0.9324	+0.0404
Recall	0.9894	0.9830	-0.0064
Precision	0.7923	0.8950	+0.1027
F1-score	0.8800	0.9358	+0.0558

4.8 Statistical Analysis

Based on the results presented in Table 6. Comparison of classification metrics before and after data augmentation, data augmentation has led to measurable improvements in the model's performance across several key metrics. Notably, accuracy increased from 0.8920 to 0.9324. The 95% confidence intervals for the original (0.8803–0.9029) and augmented (0.9292–0.9355) accuracy scores do not overlap, indicating a statistically significant improvement ($p < 0.05$) as a result of augmentation.

Table 6. Pre- vs. Post-Augmentation Performance

Metric	Original	95% CI Lower	95% CI Upper	Augmented	95% CI Lower	95% CI Upper
Accuracy	0.8920	0.8803	0.9029	0.9324	0.9292	0.9355
Recall	0.9894	0.9846	0.9930	0.9830	0.9807	0.9851
Precision	0.7923	0.7692	0.8148	0.8950	0.8893	0.9005
F1-score	0.8800	-	-	0.9358	-	-

Recall slightly declined from 0.9894 to 0.9830, but overlapping confidence intervals (original: 0.9846–0.9930; augmented: 0.9807–0.9851) suggest the change is not statistically significant. In contrast, precision significantly improved from 0.7923 to 0.8950, with non-overlapping intervals (original: 0.7692–0.8148; augmented: 0.8893–0.9005), indicating fewer false positives. The F1-score rose from 0.8800 to 0.9358, aligning with gains in precision and accuracy, though statistical significance cannot be confirmed without confidence intervals. Overall, data augmentation led to clear, statistically supported improvements in accuracy and precision while preserving strong recall, enhancing the model's performance and robustness.

5. CONCLUSION

This study developed a computer-based system for detecting aortic stenosis from X-ray coronary angiographic (XCA) images using advanced preprocessing, vessel segmentation, GAN-based key frame selection, and multiscale CNN classification. GAN-driven data augmentation improved accuracy from 89.2% to 93.2% and precision from 79.2% to 89.5%. While recall slightly decreased (98.9% to 98.3%), the F1-score rose to 93.6%, indicating better overall balance. Deployed on a compact mini-PC with a user-friendly GUI, the system shows strong potential for real-time, accessible diagnostics in clinical settings.

6. REFERENCES

[1] C. M. Otto and B. Prendergast, "Aortic-Valve Stenosis — From Patients at Risk to Severe Valve Obstruction," *New England Journal of Medicine*, vol. 371, no. 8, pp. 744–756, 2014, doi: 10.1056/nejmra1313875.

[2] D. Karelas, E. Tatsis, D. Oikonomidis, and C. H. Papadopoulos, "Diagnostic Challenges in the Management of Aortic Valve Stenosis and the Role of Imaging: A Narrative Review," *Journal of Clinical Medicine*, vol. 14, no. 4, 2025, doi: 10.3390/jcm14041231.

[3] B. A. Borlaug and E. J. Velazquez, "On Books, Covers, and Judgments in Heart Failure," *JACC: Cardiovascular Imaging*, vol. 11, no. 12, pp. 1747–1749, 2018, doi: 10.1016/j.jcmg.2017.08.021.

[4] G. Morani, B. Bolzan, S. Valsecchi, M. Morosato, and F. L. Ribichini, "Chronic venous obstruction during cardiac device revision: Incidence, predictors, and efficacy of percutaneous techniques to overcome the stenosis," *Heart Rhythm*, vol. 17, no. 2, pp. 258–264, 2020, doi: 10.1016/j.hrthm.2019.08.012.

[5] M. I. Papafaklis *et al.*, "Fast virtual functional assessment of intermediate coronary lesions using routine angiographic data and blood flow simulation in humans: Comparison with pressure wire - fractional flow reserve," *EuroIntervention*, vol. 10, no. 5, pp. 574–583, 2014, doi: 10.4244/EIJY14M07_01.

[6] R. Hurford and P. M. Rothwell, "Prevalence, prognosis, and treatment of atherosclerotic intracranial stenosis in Caucasians," *International Journal of Stroke*, vol. 16, no. 3, pp. 248–264, 2021, doi: 10.1177/1747493020974461.

[7] J. X. Xie *et al.*, "The Coronary Artery Disease-Reporting and Data System (CAD-RADS) Prognostic and Clinical Implications Associated with Standardized Coronary Co," 2018.

[8] A. J. Lansky and C. Pietras, "Fractional Flow Reserve From 3-Dimensional Quantitative Coronary Angiography Fresh Light Through an Old Window*," [Online]. Available: http://www.amednews.com/article/20120116/government/301169958/4/.

[9] J. Eckert, M. Schmidt, A. Magedanz, T. Voigtländer, and A. Schmermund, "Coronary CT angiography in managing atherosclerosis," *International Journal of Molecular Sciences*, vol. 16, no. 2, pp. 3740–3756, 2015, doi: 10.3390/ijms16023740.

[10] B. Flanagan, C. Yin, T. Suzuki, and S. Hirokawa, "Intelligent computer classification of english writing errors," *Front. Artif. Intell. Appl.*, vol. 254, pp. 174–183, 2013, doi: 10.3233/978-1-61499-262-2-174.

[11] S. Hirokawa and E. Ishita, "Non-topical classification of healthcare information on the web,"

Front. Artif. Intell. Appl., vol. 262, pp. 237–247, 2014, doi: 10.3233/978-1-61499-405-3-237.
[12] E. B. Sevandal, M. F. T. Menque, L. M. Dagsa, A. D. B. Balamad, and E. R. B. Sajonia, "Real-time IoT-based Motorcycle Accident Detection and Alert System," *Int. Exch. Innov. Conf. Eng. Sci.*, vol. 10, pp. 494–499, 2024, doi: 10.5109/7323306.